JOINT GERMAN-ISRAELI RESEARCH PROJECTS

FINAL SCIENTIFIC REPORT

German Sponsoring Agency BMBF **01 GA 9805/3**

Title of Project

DISMED Verbund : Molekulare Mechanismen der Interaktion von AD-Genen

Principal German Investigator Prof. K. Beyreuther
University of Heidelberg/ZMBH

Principal Israeli Partner Investigator Prof. Daniel Michaelson
Department of Neurobiochemistry, The George S. Wise Faculty of Life Sciences
Tel Aviv University,

Deutschsprachige Einleitung zum wissenschaftlichen Schlussbericht.

Vertraulichkeit:
Unsere Forschungen bewegen sich in einem hoch kompetitiven Feld das ein nicht unerhebliches kommerzielles Potential besitzt. Wir betrachten daher sämtliche unserer Ergebnisse, soweit sie nicht bereits als publiziert hier aufgeführt sind, als vertraulich.

Schlussbericht

- Aufgabenstellung:
Die wesentlichen mit der Alzheimer Krankheit (AD) in Zusammenhang gebrachten Gene sind das Alzheimer Vorläufer Protein (APP), die Presenilin (PS, PS1 und PS2) und das ApoE Gen. Aufgabenstellung dieses Forschungsvorhabens war es die molekulare Grundlage für die postulierte Interaktion dieser Gene/Proteine zu identifizieren.
Als grundlegendes molekulare Ereignis der AD wird heute von den meisten Forschern die übermäßige Freisetzung von Aß, bzw. Aß42, aus dem Amyloid Vorläuferprotein (APP) angesehen. Daher ist ein wesentlicher Bezugspunkt bei der Erforschung der molekularen Mechanismen der Interaktion von AD – Genen die Analyse der Auswirkung dieser Interaktionen auf die Freisetzung von Aß. Eine Verringerung dieser Freisetzung wird als grundsätzlich wünschenswert betrachtet, da dieses einen potentiellen therapeutischen Nutzen besitzt.

- Voraussetzungen unter denen dieses Projekt durchgeführt wurde:
Dieses Projekt war eine Zusammenarbeit des deutschen Partners (Konrad Beyreuther, Heidelberg) und der beiden israelischen Partner Daniel Michaelson und Reuven Stein (beide Tel Aviv). Der deutsche Partner hat sich dabei auf APP, die beiden israelischen Partner auf ApoE bzw. Presenilin fokussiert. Die entsprechenden technischen Voraussetzungen waren bei den beteiligten Labors im wesentlichen von Anfang an gegeben. Anfänglich fehlende Materialien/Ergebnisse wurden wie geplant im Laufe des Forschungsvorhabens entwickelt.

- Eingehende Darstellung der Ergebnisse:
Wissenschaftliche Darstellung siehe Anhang. Die Ergebnisse der Arbeitsgruppe Beyreuther sind in den Abschnitten B5 zu finden.
Nutzen/Verwertbarkeit der Ergebnisse: Unsere Ergebnisse belegen eine deutliche Interaktion von APP, Presenilin I, Presenilin II und Cholesterin. Dieser Zusammenhang ist bedeutend für das Verständnis der AD und hat offensichtliche Bedeutung für die Entwicklung therapeutischer Strategien. Cholesterin ist nicht nur ein essentielles Stoffwechselprodukt, sondern auch ein natürlicher Nahrungsbestandteil. Weiterhin existiert eine große Auswahl an Medikamenten welche den menschlichen Cholesterinmetabolismus beeinflussen. Es ist also prinzipiell denkbar, dass eine Lipid basierte Therapie der AD sinnvoll ist. Epidemiologische Studien weisen darauf hin, dass dieses auch beim Menschen praktikabel ist. Sowohl unsere Arbeitsgruppe, als auch eine große Zahl anderer Laboratorien haben unsere Ergebnisse zum Anlass genommen diese Interaktion weiter zu untersuchen und entsprechende Therapiemodelle zu entwickeln.

i. LIST OF FIGURES

ii. LIST OF ABBREVIATIONS

Aβ	-	Amyloid beta
AD	-	Alzheimer's disease
ApoE	-	Apolipoprotein E
APP	-	Amyloid precursor protein
CTF	-	C-terminal fragment of amyloid precursor protein
FAD	-	Familial Alzheimer's disease
LDL	-	Low density lipoprotein
LPS	-	Lypopolysaccaride
PS	-	Presenilin

1. ABSTRACT

This project centered on the study of the role of cross talk interactions between genetic risk factors of Alzheimer's disease (AD) and on examination of the extent to which such metabolic interactions may provide a unifying scheme by which patients with different genetic alterations present similar AD pathology. Accordingly, we employed cellular and animal transgenic models of the amyloid precursor protein (APP) and of the presenilins (PS) and apolipoprotein E (apoE) and focused on the pathophysiological consequence of their genotypes. The first stage of the study revealed that the pathological effects of the allele ApoE4, which is the AD risk factors, are due to increased susceptibility to neuronal injury and to impaired repair. Furthermore, we discovered that the detrimental effects of apoE were associated with a decrease in the non-amyloidogenic processing of APP. Parallel studies revealed that cholesterol stimulates the amyloidogenic processing of APP and the production of amyloid beta (Aβ). These findings suggest that the pathological effects of apoE4 and Aβ may be related to metabolic interactions between these AD genetic risk factors and that cholesterol and brain lipids play an important role in these interactions. These basic findings have important clinical ramifications which we are planning to jointly pursue in the future.

2. CONCLUSIONS

1. The apoE4 genotype increases susceptibility to head injury whereas apoE3 ehances repair.
2. ApoE3 stimulates astrogliosis isoform specifically following LPS induced brain inflammation whereas the apoE4 and apoE deficiency genotypes lack this activity.
3. Non amyloidogenic processing of APP following head injury is activated isoform specifically by apoE3 and not by apoE4.
4. Overexpression of PS does not trigger apoptosis.
5. PS2 is a modulator of protein synthesis.
6. *In vivo* and *in vitro* treatments which lower neuronal cholesterol levels reduce amyloid-beta levels.
7. Cholesterol depletion lowers amyloidogenesis by parallel and independent effects on β- and γ-secretase.

3. PUBLICATIONS (Israeli partners)

1. Lomnitski, L., Chapman, S., Hochman, A., Kohen, R., Shohami, E., Chen, Y., Trembovler, V. and Michaelson, D.M.(1999) Altered antioxidant mechanisms in apolipoprotein E-deficient mice prior to and following closed head injury. Biochem. Biophys. Acta 1453: 359-368.

2. Lomnitski, L., Oron, L., Sklan, D. and Michaelson, D.M. (1999) Distinct alterations in phospholipid metabolism in brains of apolipoprotein E-deficient mice. J. Neuroscience Research 58: 586-592.

2. Genis, I., Shohami, E. and Michaelson, D.M. (2000) Tau hyperphosphorylation in control and apoE-deficient mice following head injury. J. Neurosc. Res. 60: 559-564.

4. Chapman, S., Sabo, T., Roses, A.D. and Michaelson, D.M. (2000) Reversal of presynaptic deficits of apolipoprotein E-deficient mice in human apolipoprotein E transgenic mice. Neuroscience 97: 419-424..

2. Sabo, T., Lomnitski, L., Nyska, A., Beni, S., Maronpot, R.R., Shohami, E., Roses, A.D. and Michaelson, D.M. (2000) The susceptibility of transgenic mice expressing human apolipoprotein E to closed head injury: The allele E3 is neuroprotective whereas E4 increases fatalities. Neuroscience 101: 879-884.

3. Gamliel, A., Teicher, C., Michaelson, D.M., Pradier, L., Hartmann, T., Beyreuther, K. and Stein, R. (2002) Increased expression of presenilin 2 inhibits protein synthesis. Neuroscience 19: 111-124.

7. Ophir, G., Meilin, S., Efrati, M., Chapman, J., Karussis, D., Roses, A. and Michaelson D.M. Astrocyte activation *in vivo* is modulated isoform-specifically by apolipoparotein E3 but not by apolipoprotein E4. Neuroscience (Submitted).

8. Ezra, Y., Oron, L., Roses, A.D., Beni, S.M., Shohami, E. and Michaelson, D.M. Isoform-specific effects of apolipoprotein E on secretion of the amyloid precursor protein following closed head injury. J. Neurochemistry (Submitted).

A. INTRODUCTION

The overall objective of this project is to study the molecular mechanisms underlying the cross talk between genetic molecular hallmarks of familial and sporadic Alzheimer's disease (AD) and to examine the extent to which such metabolic interactions may provide a unifying, mechanistic scheme which could explain how patients with different genetic alterations present similar AD neuropathology and phenotype.

In view of the importance of intracellular trafficking and membrane sorting in neuronal function, the experiments focus on the extent to which cross talk interactions between genetic molecular hallmarks of AD such as the amyloid precursor protein (APP), apoE and presenilin (PS) are affected by membrane-dependent mechanisms. The following results were thus obtained:

B. RESULTS
B1-B4 Israeli partners
B5 german partner

B1. The effects of apoE on neuronal maintenance

Apolipoprotein E (apoE)-deficient mice provide a useful system for studying the role of apoE in neuronal maintenance and repair. Previous studies revealed specific memory impairments in these mice which are associated with presynaptic derangements in projecting forebrain cholinergic neurons. In the present study we examined whether dopaminergic, noradrenergic and serotonergic projecting pathways of apoE-deficient mice are also affected, and investigated the mechanisms which render them susceptible. The densities of nerve terminals of forebrain cholinergic projections were monitored histochemically by measurements of acetylcholinesterase activity whereas those of the dopaminergic nigro-striatal pathway, the noradrenergic locus coeruleus cortical projection and the raphe-cortical serotonergic tract were measured autoradiographically utilizing radioligands which bind specifically to the respective presynaptic transporters of these neuronal tracts.

The results obtained revealed that synaptic densities of cholinergic, noradrenergic and serotonergic projections in specific brain regions of apoE-deficient mice are markedly lower than those of controls. Furthermore, the extent of presynaptic derangement within each of these tracts was found to be more pronounced the further away the nerve terminal is from its cell body. In contrast the nerve terminal density of the dopaminergic neurons which project from the substantia nigra to the striatum was unaffected and was similar to that of the controls. The rank order of these presynaptic derangements at comparable distances from the respective cell bodies was found to be septohippocampal-cholinergic > nucleus basalis-cholinergic > locus coeruleus-adrenergic > raphe-serotonergic >> nigrostriatal-dopaminergic. Interestingly, this rank order is similar to that observed in AD. These results suggest that two complementary factors determine the susceptibility of brain projecting neurons to apoE deficiency: pathway-specific differences and the distance of the nerve terminals from their cell body.

Further experiments which utilized mice transgenic for either human apoE3 or human apoE4 revealed that the brain neuronal deficits induced by apoE deficiency were similarly ameliorated in both the apoE3 and the apoE4 transgenic mice. These findings suggest that the isoform specificity of the apoE dependent brain neurons is not phenotypically expressed at a young age under non challenging conditions. Accordingly and as described in the following chapter, we investigated the effects of the apoE genotype on neuronal and brain susceptibility to brain injury.

B2. The effects of apoE genotype on neuronal susceptibility to closed head injury

The susceptibilities of the apoE3 and apoE4 transgenic mice and of apoE-deficient and normal control mice to close head injury (CHI) were assessed by measurements of their neurological status during 11 days following head injury and by monitoring the number of mice which have died in each group.

Four control, 6 apoE-deficient and 5 apoE3 transgenic mice died within 11 days following CHI, numbers corresponding to the same percentages of mice out of the total, in each of these groups (i.e., respectively 27%, 30% and 36%). In contrast 56% of the apoE4 transgenic mice (i.e., 10 out of a total of 18 mice) died within 11 days following CHI. This difference between the extents of mortality of the apoE4 transgenic mice and the other groups was statistically significant ($p<0.002$ X^2 test for comparisons between the apoE4 transgenic mice and the control and $p<0.02$ for comparison between the apoE4 transgenic mice and either the apoE3 transgenic mice or the apoE-deficient mice).

The neurological status of the surviving CHI mice was evaluated by using the Neurological Severity Score (NSS) at different time intervals following injury. The apoE3 and apoE4 transgenic mice and apoE-deficient and normal control mice displayed similar NSS values at 1 hour (respectively, 6.7 ± 0.6; 6.1 ± 0.4; 6.0 ± 0.7; 6.9 ± 0.7), indicating similar severity of injury. Differences in the extents of recovery of the different groups were, however, remarkable by 3 days post- injury, such that the NSS scores of the apoE3 transgenic mice were lower than those of the other three groups (e.g., NSS of 3 ± 0.7 vs. corresponding NSS values in the range of 5 - 6 for the other three groups). This facilitated recovery of the apoE3 group sustained until at least day 11. Statistical analysis of the NSS data revealed significant differences between the four groups at days 3 and 11 post-injury (one-way ANOVA; respectively, $F(3/38) = 3.27$; $p<0.05$ and $F(3/38) = 6.0$ ($p<0.02$). This result was associated with a significant reduction of the NSS scores of the apoE3 transgenic mice relative to both the control and apoE-deficient mice ($p<0.03$ at day 3 and $p<0.002$ at day 11). In contrast, there were no significant differences between the NSS values of the apoE4 transgenic mice and those of the control and apoE-deficient mice.

The difference between the NSS values of the apoE3 and apoE4 transgenic mice at 3 days (respectively 3 ± 0.7; 4.9 ± 0.8) and at 11 days post-injury (respectively 2.6 ± 0.6; 4.1 ± 0.8) reflected P values of 0.06 and 0.07. Since the number of mice in the injured apoE4 transgenice group was smaller than those in the other groups, due to a higher mortality rate, the NSS data of the four mice groups were further analyzed by one-way repeated ANOVA (group x days). This analysis also revealed a significant difference between the NSS values of the four groups (ANOVA $F(3/38) = 2.8$; $p<0.05$) which, in addition to a significant decrease in the NSS values of the injured apoE3

transgenic mice relative to the control and apoE-deficient mice ($p<0.002$), was also associated with a significant decrease relative to the apoE4 transgenic mice ($p<0.05$).

Coronal histological sections of the plane of impact of apoE3 and apoE4 transgenic mice and of control and apoE-deficient mice 11 days post-CHI revealed that CHI resulted in brain damage in all mice. Inflammation, hemorrhage and edema occurred and resulted in the loss of a significant fraction of the brain parenchyma; the magnitude of this loss was maximal at the plane of injury. The size of the damaged brain areas of the control and apoE-deficient mice was comparable; whereas, that of the CHI apoE3 transgenic mouse was markedly smaller. The size of the damaged brain area of the injured apoE4 transgenic mouse was also larger than that of the injured apoE3 transgenic mouse but was somewhat smaller than that of the injured control and apoE-deficient mice. Quantitative analysis of the relative extents of brain damage of head-injured mice (respectively n = 15, 19, 13 and 11 brains of control, apoE-deficient, apoE3 and apoE4 transgenic mice) revealed a significant difference between the extent of brain damage of the four mice groups (one way ANOVA; $F(3/55) = 2.89$; $p<0.05$). This difference was associated with a significant reduction in the extent of brain damage of the injured apoE3 transgenic mice to 40 ± 5% of that of the injured controls. In contrast, there were no statistically significant differences between the extents of brain damage of the injured apoE4, apoE-deficient and control mice. These results are in accordance with the neurological findings and support the suggestion that the apoE3 transgenic mice recover more effectively from CHI than the other mouse groups.

In conclusion, this study revealed that mice transgenic for human apoE4, which is the AD risk factor, are more susceptible to CHI than human apoE3 transgenic mice. Furthermore, the findings obtained revealed that the apoE3 transgenic mice recovered more rapidly from CHI than control, apoE-deficient and apoE4 transgenic mice, and that the infarct size of the injured apoE3 mice was significantly smaller than that of the other mouse groups. In contrast, analysis of the fatalities following CHI revealed that a similar fraction of the apoE3, control and apoE-deficient mice died following injury (27 - 36% within the first 11 days); whereas, a significantly higher number of the apoE4 mice (56%) died during this time period. These findings suggest that apoE3 has a neuroprotective effect which results in better recovery and lower brain damage of the animals which survive following CHI; whereas apoE4, which is the AD risk factor, has a detrimental effect which increases the number of fatalities. It is not yet known whether the protective effects of apoE3 are due to truly 'neuroprotective' effects, namely rescue of neurons, or to indirect effects on non-neuronal systems, such as the inflammatory response, which in turn affects the neurons.

B3. The mechanisms underlying the effects of apoE on neuronal maintenance and repair

B3.1. Inflammatory mechanisms

These experiments investigated the possibility that brain inflammatory responses, in particular microgliosis and astrogliosis, are affected by the apoE genotype. This was pursued by intracerebroventricular (i.c.v.) injection of LPS into brains of transgenic mice expressing either human apoE3 or apoE4 on a null mouse apoE background, followed by immunohistochemical comparisons of the resulting extents of activation of brain microglia and astrocytes.

Injection of LPS i.c.v. into brains of 6 months' old control C57BL/6J mice resulted in a marked, immunohistochemically detectable activation of microglia and astrocytes. This effect was time- and LPS dose-dependent. Maximal microglia and astrocyte activation was observed in the hippocampus 3 days after the i.c.v. injection of 500 ng LPS and the numbers of activated microglial cells and astrocytes thus obtained (respectively 97 ± 18 and 132 ± 12 cells per mm^2; n = 5) were markedly higher than those of either sham treated (respectively 41 ± 9 and 84 ± 9 cells/mm^2; $p<0.01$, n = 5) or naive non-treated control mice (respectively 15 ± 9 and 32 ± 10 activated cells per mm^2; n = 5). The levels of activated brain microglia and astrocytes in all subsequent experiments were therefore monitored in the hippocampus and at day 3 after the i.c.v. injection of 500 ng LPS.

The effects of apoE and of apoE genotype on LPS-stimulated activation of brain microglia and astrocytes were first investigated in 6 month' old transgenic mice which express either human apoE3 or human apoE4, and in age-matched apoE-deficient and control mice. Two way ANOVA of the results thus obtained revealed a significant effect of group ($F(3.47) = 8.54$, $p<0.001$) and treatment ($F(147) = 13.37$, $p<0.001$) and a marginally significant effect of group x treatment ($F(3.47) = 2.38$; $P = 0.08$). Further examination of the results revealed that the levels of activated astrocytes of the four sham treated groups were similar but that, following LPS treatment, they differed markedly. Utilizing a stringent t-test criterion of $p<0.001$ revealed that LPS treatment resulted in significant activation of brain astrocytes in the control and apoE3 transgenic mice (respectively 132 ± 12 and 126 ± 10 activated astrocytes/mm^2; $p <0.001$), but had no effect on the apoE-deficient and the apoE4 transgenic mice (respectively 84 ± 26 and 71 ± 27 activated astrocytes/mm^2). Measurements of the levels of activated microglia in the four mice groups revealed a significant effect of treatment ($F(1.48) = 3.185$; $p<0.001$) but no effect of either group ($F(3.48) = 0.99$; $p>0.4$) or group x treatment ($F(3.48) = 0.9$; $p>0.4$) on microglial activation. Further examination of the results revealed that all of the four sham treated groups had similar levels of activated microglia and that LPS stimulated gliosis in the control, apoE deficient and apoE4 transgenic mice (respectively 97 ± 18; 98 ± 40; 92 ± 39 activated microglia/mm^2)) was statistically significant relative to the corresponding sham treated groups ($p<0.01$). A small increase was also observed in the apoE3 transgenic mice following treatment, but it was not statistically significant.

Brain neuropathology in apoE-deficient and in apoE4 transgenic mice is age-dependent and becomes prominent at about one year. We therefore examined the LPS response in 12 months' old mice and compared it to that observed in the younger animals. The levels of astrocyte activation thus obtained revealed significant effects of group ($F(3.39) = 3.63$; $p<0.02$) and treatment ($F(2.39) = 23$, $p<0.001$) and of the interaction between group x treatment ($F(3.39) = 7.19$; $p<0.01$). Further analysis of these results revealed that LPS increased the levels of activated astrocytes of 12 months' old apoE-deficient and apoE4 transgenic mice to a significant and similar extent (respectively 128 ± 16 and 138 ± 19 activated astrocytes/mm^2; $p<0.001$) but had no effect on those of the control and apoE3 transgenic mice. Thus, whereas the 12 months' old apoE-deficient and the apoE4 transgenic mice had a marked astrocytic response to LPS and the 6 months' old mice did not, the control and apoE3 transgenic mice both yielded opposite, age-dependent responses. Measurement of the numbers of activated microglia following i.c.v. injection of LPS to 12 months' old mice showed no differences between the mice groups ($F(3.41 = 1.08$; $p>0.35$) and a marginal effect of

treatment ($F(1.41) = 3.02$; $p<0.09$) and of the interaction between group and treatment ($F(3.41 = 2.3$; $p<0.09$). Thus, the extent of microglial activation following LPS treatment decreases with age but, unlike astrocyte activation, is not affected by either apoE deficiency or the human apoE transgenes in both the 6 and 12 months' old mice.

Immunohistochemical staining of brain sections of the apoE transgenic mice for human apoE revealed LPS-dependent elevation of apoE-positive cells in the hippocampus of 6 months' old apoE3 and the apoE4 transgenic mice; a similar finding was observed in 12 months' old transgenic mice. In both age groups the levels of apoE-positive cells of the apoE4 transgenic mice were comparable but somewhat higher than those of the corresponding apoE3 transgenic mice.

In conclusion, the present experiments revealed that the brain inflammatory response following i.c.v. injection of LPS depends on the presence and genotype of apoE and is age-dependent. Accordingly, LPS treatment of 6 months' old control and apoE3 transgenic mice, but not of age-matched apoE-deficient and apoE4 transgenic mice, resulted in marked and significant activation of brain astrocytes. Opposite results were observed in 12 months' old mice where the same LPS treatment triggered astrocytic activation in apoE-deficient and apoE4 transgenic mice, but not in control and apoE3 transgenic mice. In contrast, LPS-dependent microglial activation was not affected either by apoE deficiency or by the presence of human apoE3 and apoE4. These results show that apoE plays an age-dependent regulatory role in the activation of brain astrocytes which can be either excitatory or inhibitory (e.g. 6 vs. 12 months' old mice). Furthermore, these effects are mimicked by human apoE3 but not by the apoE4 allele, which yields a phenotype similar to that of apoE deficiency. The loss of LPS-mediated activation of astrogliosis in the apoE4 transgenic mice is not due to lack of brain apoE in these mice which, following stimulation with LPS, produce similar brain apoE levels to those of the apoE3 transgenic mice.

B3.2. Cross talk between apoE and tau

In the present experiments we investigated the possibility that the phenotypic effects of the apoE genotype are mediated by cross talk interactions with the cytoskeletal protein tau. This was performed by investigation of the effects of apoE deficiency and of the human apoE isoforms on the level and extent of tau phosphorylation prior to and following head injury. Accordingly, we first focused on examination of the effects of head injury on control and apoE deficient mice.

This revealed that, prior to head injury, tau of apoE-deficient mice contains a hyperphosphorylated 'hot spot' domain that is localized N-terminally to the microtubule binding domain of tau. Closed head injury resulted in transient hyperphosphorylation of epitopes in the 'hot spot' domain whose extent and time course in the two mice groups varied markedly. Tau hyperphosphorylation in the injured controls was maximal by about 4 hours following injury and returned to basal levels by 24 hours. By contrast, almost no tau hyperphosphorylation was observed in the apoE deficient mice at 4 hours after injury. Some tau hyperphosphorylation was however observed in the head injured apoE-deficient mice at longer time intervals. The extent of this hyperphosphorylation was markedly lower than that maximally observed in the injured controls. However, for some of the 'hot spot' epitopes of the apoE deficient mice, it was still apparent one week after injury. These findings show that the chronic neuronal impairments brought

about by apoE deficiency and acute response to head injury are both associated with hyperphosphorylation of the same tau domain and that apoE deficient mice have impaired ability to generate acute tau hyperphosphorylation response to head injury.

Further support for the assertion that tau hyperphosphorylation is a general indication of neuronal stress and is not directly coupled to apoE was obtained by experiments which revealed that tau hyperphosphorylation associated with apoE deficiency is similarly ameliorated in both the apoE3 and the apoE4 transgenic mice.

B3.3. Cross talk interactions between apoE genotype and amyloid precursor protein

These experiments examined the possibility that cross talk interactions between apoE and the amyloid precursor protein (APP) play a role in the pathophysiological effects of the apoE genotype.

Immunoblot measurements of the brain levels of APP and of its soluble fragment APPs revealed that they were slightly lower in apoE4 transgenic mice than in apoE3 transgenics, whose levels were similar to those of control and apoE-deficient mice. Closed head injury increased the levels of brain APPs of control mice. Similar increases were observed with the apoE4 transgenic and the apoE-deficient mice, whereas the brain APPs levels of the apoE3 transgenic mice increased much more markedly following head injury.

Cell culture studies utilizing neuroblastoma N2a cells revealed that the secretion of APPs is stimulated by the addition of apoE4 but not by apoE3. This isoform-specific effect of apoE4 was inhibited by low levels of either RAP (5 nM) or lactophorin (10 μg/ml) which, under these conditions, inhibit LRP receptor mediated processes. By contrast, higher levels of RAP (500 nM), which inhibit LDL receptor-mediated processes, enhanced the effects of apoE4 on APPs secretion.

These *in vivo* and *in vitro* findings suggest that the acute and chronic pathological effects of apoE4 may both be affected by cross talk interactions between apoE and APP and that these effects are mediated by several types of brain apoE receptors.

B3.4. The effects of apoE genotype on brain lipid metabolism

These experiments investigated the possibility that the pathophysiological effects of distinct apoE genotypes are related to isoform-specific effects of apoE on brain lipid metabolism. This was performed by measurements of the effects of apoE genotype on the cholesterol and phospholipid levels of neuronal brain membranes of AD patients and controls and by parallel measurements of the effects of apoE genotype on the brain lipids of human apoE3 and apoE4 transgenic mice.

(i) Brain lipids of Alzheimer's disease patients and controls. Analysis of the lipid composition of brain synaptosomal membranes (fraction P_2) of normal controls homozygous for apoE3 (control 3/3) revealed that they contain similar levels of cholesterol and phospholipids (respectively 927±37 and 925±54 nmole/mg protein;

means ± S.E.M.; n=5) and that their phospholipids comprised of PC (33.1± 0.9%), PE (21.5±1.6%), PPE (18.2±1.8%), PS (15.2± 0.3%), PS (4.2±0.3%) and SM (7.6±0.8%).

Measurements of the brain lipid composition of AD patients homozygous for apoE3 (AD 3/3) revealed a marginally significant decrease of 10.5±3.5% in cholesterol levels compared to that of controls with the same genoptype (p=0.09) but that both groups had similar total phospholipid levels. Comparison of the phospholipid compositions of these groups revealed no differences in the levels of PC, PS, PI and SM. There was however a small difference in the levels of ethanolamine containing phospholipids, such that PE levels were slightly lower in the AD 3/3 group than in the control 3/3 subjects, whereas the opposite was observed with PPE. Further analysis of these results in terms of the percentage of PPE and of the total ethanolamine-containing lipids revealed that it was 45.7 ±4.4% in the control 3/3 samples and 50.7±2% in the AD 3/3 samples. These differences however were not statistically significant. Measurements of the brain lipid composition of AD patients homozygous for apoE4 (AD 4/4) revealed that the cholesterol content of the P_2 membranes was intermediate to those of the apoE3 homozygous AD and controls and that their phospholipid levels were slightly but not significantly lower than those of both groups. Furthermore, there were no differences in the phospholipid compositions of the AD 3/3 and AD 4/4 cases and the slight elevation, relative to control 3/3, in the fraction of PPE from the total ethanolamine-containing lipids was similar in the AD 4/4 and AD 3/3 groups.

Analysis of the fatty acid composition of control 3/3 brain phospholipids revealed that C16:0 which comprises over 40% of the PC was replaced in the other lipids by C18:0 and C18:1 and by considerable levels of polyunsaturated fatty acids. Analysis of the brain fatty acid compositions of AD 3/3 and AD 4/4 revealed no differences in those of PC, PE and PI of the three groups and of their SM. There were, however, small differences in the fatty acid composition of PPE and PS of the three groups, such that the levels of C22:6 were increased in AD (AD 4/4 > AD 3/3 > control 3/3) and those of C18:1 were decreased (AD 4/4 < AD 3/3 < control 3/3). The difference between the C22:6 levels of PS of the AD 4/4 and the control 3/3 cases were marginally significant (p=0.06), whereas the other differences were not.

(ii) Brain lipids of apoE transgenic mice. The effects of apoE on brain lipid composition were also studied utilizing mice which are either apoE-deficient or trasngenic for human apoE3 and apoE4. Comparison of the brain lipids of control and apoE-deficient mice revealed non significant decreases in the cholesterol, PC, PE and PS levels of the synaptosomal membranes (fraction P_2) of the apoE-deficient mice relative to the controls. In contrast, there was a marked decrease in cholesterol (32±3%), PE (31± 4%) and PI (28±3%) in the microsomal membranes (fraction P_3) of the apoE-deficient mice relative to the controls ($p < 0.05$) and a less pronounced decrease in PC and PS levels. These findings are in accordance with results previously obtained with another strain of apoE-deficient mice and suggest that intracellular membranes are affected preferentially by apoE. The extent to which the effects of apoE deficiency on microsomal lipids are reversed in apoE transgenic mice was examined. This revealed that the human apoE3 and apoE4 transgenes partially and similarly reversed the decreases in cholesterol PE and PI levels brought about by apoE deficiency. Measurements of the fatty acid composition of the different microsomal phospholipids revealed that they were unaffected either by apoE deficiency or by the human apoE transgenes.

In conclusion, the present AD and animal model findings suggest that the pathological effects of the apoE genotype are not associated with changes in the overall lipid composition of brain neuronal membranes. However, the possibility that the lipid composition and trafficking of specialized subcellular compartments are affected isoform-specifically by apoE cannot be excluded.

B4. The role of Presenilins in neuronal function

B4.1. Cross talk between presenilins and the apoptotic machinery

It was suggested that presenilin (PS) may be involved in apoptosis. The exact role of PSs in apoptosis is not clear yet. Some of the published data suggest that both PSs_{WT} and PSs_{mut} induce apoptosis, while others suggest that the function of PSs_{WT} such as $PS1_{WT}$ is to inhibit whereas PSs_{mut} lost this function or gained a new pro-apoptotic function. Moreover some studies suggest that overexpression of PSs is suficient by itself to induce apoptosis other sugest that it only increase cell suceptibility to apoptosis.

Accumulating evidence suggests that PS expression in the brain is increased in some cases of AD and that apoptosis may play a role in the neuronal death that occurs in AD. In view of the above, we undertook to study the mechanism of action of overexpressed PS2 on apoptosis. For this purpose cells were co-transfected with PS2 and cell viability was monitored.

Expression and Subcellular Distribution of Overexpressed PS2 Proteins in CHO and 293T cells—To determine whether the overexpressed PS2 proteins exhibit similar properties to those of the endogenous proteins, the expression and subcellular distribution of overexpressed PS2 proteins in CHO and 293T transfected cells were examined by confocal immunofluorescence microscopy (Fig. 1A) and by Western blot analysis (Fig. 1B). The overexpressed PS2wt and PS2mut proteins exhibited a perinuclear network labeling pattern consistent with a predominantly intracellular localization in the ER and Golgi. These findings thus suggest that the subcellular distribution of the exogenously expressed PS2 proteins is similar to that described for endogenous PS2. In addition, as shown by Western blot analysis (Fig. 1B), the apparent molecular weights of the overexpressed PS2 proteins in the 293T cells and the endogenous proteins were similar. As protein accumulation in the ER could lead to cell stress, we examined the effect of PS2 overexpression on the steady-state levels of Bip/GRP78, a luminal ER-resident protein induced by accumulation of misfolded ER proteins. As shown in Fig. 1B, overexpression of either PS2wt or PS2mut in 293T cells (which are transfected very efficiently) did not affect the amounts of Bip/GRP78 protein, whereas this protein was increased by treatment with tunicamycin and thapsigargin, two effective inducers of ER stress. These results thus suggest that overexpression of human PS2 proteins in these cells does not cause ER stress.

Overexpression of Human PS2 does not induce Apoptosis—In an attempt to investigate the possible role of PS2 in apoptosis, we employed a method in which PS2 is co-expressed with a reporter gene. In this technique the death effect of an apoptotic gene is detected and monitored by examining the expression of the co-transfected reporter gene. Mammalian expression vectors containing cDNAs for human PS2wt and PS2mut were transiently co-transfected into CHO cells with the reporter gene GFP. The

expression of these genes was determined by GFP fluorescence and by immunofluorescence labeling using anti-PS2 antibodies. As shown in Fig. 1C, almost all PS2-positive cells were also GFP positive, indicating that individual transfected cells had acquired and were expressing both PS2 and GFP genes. These findings support the suitability of co-transfection as a method of co-expressing both exogenous genes in the same cell.

To determine whether PS2 overexpression can induce apoptosis, CHO cells and N2a neuroblastoma cells were co-transfected with GFP and empty vector (pcDNA3), PS2wt or PS2mut, as well as with the positive control, Bax, a pro-apoptotic member of the Bcl-2 family that induces apoptosis upon overexpression. As shown in Fig. 2A, cells co-transfected with GFP and PS2wt, PS2mut, or Bax exhibited a marked reduction in the expression of GFP (as indicated by the intensity of GFP fluorescence) compared to cells co-transfected with GFP and pcDNA3. Determination of the total number of GFP-positive cells in these cultures, regardless of differences in their intensities (under sensitive conditions in which cells with low GFP content could also be detected), revealed however that the number of GFP-positive cells in PS2wt and PS2mut cultures was not smaller than that in pcDNA3-transfected cultures (data not shown) and was not accompanied by cell death. In contrast, in the Bax-transfected culture the number of GFP-positive cells was significantly smaller and was accompanied by the appearance of dead cells [small and fragmented cells (Fig. 2A*,* phase contrast image)]. Taken together, these findings suggest that although overexpression of PS2wt or PS2mut in CHO or N2a cells reduces the intensity of the co-expressed GFP, this reduction is not accompanied by cell death. To directly assess whether overexpression of PS2 induces apoptosis, we examined CHO or 293T cultures co-transfected with GFP and pcDNA3, PS2wt, PS2mut, or Bax for the presence of apoptotic cells. As indicated in the DNA histograms obtained by flow cytometric analysis of GFP-positive CHO-transfected cultures (Fig. 3A), the percentage of GFP-positive cells exhibiting degraded DNA content (a characteristic feature of apoptotic cells) was low and similar in cultures transfected with pcDNA3, PS2wt, or PS2mut (4.3, 4.5, or 6.9% respectively), and was much higher (17%) in Bax-transfected cultures. 293T cells co-transfected with GFP and pcDNA3, PS2wt, PS2mut, or Bax were examined for GFP expression and for the presence of apoptotic cells by staining the cells with Hoechst 33342, a DNA-specific fluorescent dye. As shown in Fig. 3B, the number of 293T cells exhibiting a high GFP content was much lower in PS2wt, PS2mut, and Bax-transfected cultures than in cultures transfected with pcDNA3, whereas apoptotic cells exhibiting chromatin condensation and fragmentation were detected only in cultures transfected with Bax. Similar results were obtained in CHO cells transfected with the above mentioned vectors and stained with Hoechst 33342 (data not shown). Taken together, these results demonstrate that overexpression of either PS2wt or PS2mut inhibits expression of the co-transfected reporter gene without concomitant induction of apoptosis.

Previously it was shown that staurosporine induces a 10-fold increase in caspase-3 activation in PS1mut compare to PS1wt-expressing human H4 neuroglioma cells [Kovacs, 1999 #6174] suggesting that PSs may induce or potentate caspase activation. To further explore the effect of overexpression of PS2 on the apoptotic machinery, we determined the effect of PS2wt and PS2mut on caspase-3 activation. CHO cells were co-transfected with GFP and pcDNA3, PS2wt, PS2mut, or Bax and caspase-3 activation in transfected cells was determined by staining the cells with CM1 antibody, which recognizes the p18 subunit of cleaved caspase-3[Srinivasan, 1998

#6362]. As shown in Fig. 4, in pcDNA3, PS2wt or PS2mut there were only very few, if any, GFP positive cells that were stained also with the CM1 antibodies, whereas in Bax-transfected cells most GFP positive cells (which were also apoptotic) were stained with the CM1 antibodies. These results suggest that overexpression of PS2 in CHO cells does not induce neither caspase-3 activation nor apoptosis.

Next we examined whether in addition to inhibiting GFP expression, overexpression of PS2wt or PS2mut would also inhibit the expression of other co-transfected reporter genes. CHO and N2a cells were co-transfected with the reporter gene luciferase and pcDNA3, PS2wt or PS2mut expression vectors. As shown in Fig. 2B, overexpression of PS2wt or PS2mut in CHO or N2a cells inhibited luciferase activity in PS2wt- and PS2mut- transfected cells compared to cells transfected with the control vector pcDNA3. The effect of PS2wt or PS2mut on the co-expressed reporter gene was slightly stronger in CHO cells, and these cells were therefore used in the subsequent experiments.

B4.2 Presenilin 2 is a Modulator of Protein Synthesis

In view of the finding that overexpression of PS2wt or PS2mut inhibits the expression of the co-expressed reporter gene, we next examined whether PS2wt and PS2mut differ in their ability to mediate this effect. We also determined the specificity of this effect, in particular in comparison to the effect of PS1. CHO cells were co-transfected with the reporter gene luciferase and increasing concentrations of PS2wt or PS2mut plasmids.

Comparison of the Effects of PS2mut and PS2wt on the Co-expressed Reporter Gene— Western blot analysis revealed that PS2wt and PS2mut were expressed in the transfected cells in similar amounts and in a dose-dependent manner (data not shown). As shown in Fig. 4, co-transfection of luciferase with either PS2wt or PS2mut induced a dose-dependent inhibition of luciferase activity. Statistical analysis revealed a tendency for the effect of PS2mut to be higher than that of PS2wt, but this difference was only marginally significant ($F[1,37] = 2.9$, $p < 0.1$). To examine the specificity of the effect of PS2 overexpression on the co-expressed reporter gene, we examined the effects of two additional ER-resident transmembrane proteins, the human PS1wt protein (which is highly homologous to PS2 protein) and the integral ER membrane protein HMG–CoA reductase (HMGR), on the co-expressed luciferase gene. As shown in Fig. 4, overexpression of PS1wt was not effective at low plasmid concentrations (0.1–0.4 μg). At higher concentrations it produced an inhibitory effect on luciferase activity, but this effect was much weaker than that of PS2 at the same concentration range (0.8–1.2 μg). Similar results were obtained with PS1mut (data not shown). Co-expression of HMGR with the reporter gene luciferase had no effect on luciferase activity at any of the concentrations tested. The above three proteins (HMGR, PS1 and PS2) were all shown to be expressed in the transfected cells (data not shown). Taken together, the results show that the inhibitory effect of PS2 on the co-expressed reporter gene is specific and that the effect of PS2mut is marginally stronger than that of PS2wt.

Direct Demonstration that Overexpression of PS2wt and PS2mut Leads to Inhibition of Protein Synthesis—The inhibitory effect induced by PS2 (and perhaps PS1) proteins on the expression of the co-expressed reporter gene may be attributed to

the effect of PS2 on transfection efficiency, transcription, or protein translation and degradation. To distinguish between these possibilities we first examined whether overexpression of PS2 reduces the amount of the reporter mRNA. The amounts of GFP mRNA and protein were determined in CHO cultures co-transfected with GFP and PS2wt, PS2mut, PS1wt, or PS1mut. As shown in Fig. 5, the amounts of GFP mRNA in each transfected culture were similar, whereas GFP was present in much smaller amounts in PS2 (PS2wt or PS2mut)-transfected cultures than in pcDNA3 and PS1 (PS1wt or PS1mut)-transfected cultures. The ratio of GFP protein to GFP mRNA was much lower in PS2-transfected cultures than in cultures transfected with either the control vector pcDNA3 or PS1. However, this ratio was lower in cultures transfected with PS1 than in those transfected with pcDNA3. Taken together, these results demonstrate that PS2 overexpression does not affect the amounts of the reporter mRNAs expressed, and thus suggest that the effect of PS2 proteins on the expression of the reporter genes is mediated via its effect on the synthesis or stability of the reporter protein.

In an attempt to determine directly whether PS2 proteins inhibit translation of the co-expressed reporter mRNA we examined the distribution of GFP mRNA between monosomes and polysomes after transfection, since translationally inactive mRNAs are present as free cytoplasmic monosomes whereas actively translated mRNAs are contained within polysomes. Accordingly CHO cells were transfected with either PS2mut or pcDNA3 vectors, and sucrose density gradients were used to separate monosomes from polysomes. Representative profiles of such separation obtained from PS2mut and pcDNA3 transfected cultures are shown in Fig. 6A. It should be noted that the two transfected cultures exhibited similar polysomal profiles, but the ratio of polysomes to monosomes in the profile obtained from PS2mut transfected cells was slightly lower (by 15%) than that obtained from pcDNA3 transfected cells. Since these profiles represent monosomes and polysomes obtained from the total cell population (and not just the transfected cells), a large difference in the distribution of the total monosomes and polysomes is not expected. The different ribosomal fractions were combined into two fractions, the monosomal (40S, 60S and 80S) and the polysomal fractions, as indicated in Fig. 6A. Total RNA from each of these two fractions was extracted and the amount of GFP mRNA in each fraction was determined by Northern blot analysis. As shown in Fig. 6B and C, most of the GFP mRNA isolated from pcDNA3-transfected cells was associated with the polysomes (polysomal to monosomal GFP mRNA ratio ~ 3), whereas in PS2mut-transfected cells there was a substantial reduction in the amount of GFP mRNA associated with polysomes and an increase in the amount associated with monosomes (polysomal to monosomal GFP mRNA ratio ~ 1.5). Since the extent to which an mRNA associates with ribosomes indicates its level of translation, the results depicted in Fig. 6 demonstrate that overexpression of PS2 leads to inhibition of translation of the co-transfected reporter gene.

The possibility that PS2 proteins can also inhibit translation of the reporter protein by reducing its stability was examined by measuring the rate of degradation of the co-transfected luciferase reporter protein in cultures co-transfected with luciferase and pcDNA3, PS2wt, or PS2mut vectors. The protein synthesis inhibitor cyclohexamide (1 μM) was added to the cultures 24 h after transfection, and luciferase activity in each transfected culture was determined 4, 6, and 8 h later. The degradation rates of luciferase (indicated by the reduction in its activity at the indicated time points) were similar in cultures transfected with pcDNA3 and PS2 vectors (data not shown). These

findings show that PS2 overexpression does not accelerate the rate of degradation of the co-expressed reporter protein, and thus — together with the findings showing that the amount of GFP mRNA in PS2 transfected cultures was similar to that of control transfected cultures and that PS2 overexpression reduced the polysomal distribution of GFP mRNA — suggest that overexpression of PS2 inhibits translation of the co-expressed exogenous gene.

Next we examined whether overexpression of PS2 also inhibits the synthesis of endogenous proteins. CHO cells were transfected with PS2wt, PS2mut, PS1wt, or pcDNA3 vectors. As a positive control, cells were also transfected with an expression vector that directs the expression of interferon-inducible RNA-dependent protein kinase (PKR), a well known inhibitor of translation (53). As shown in Fig. 7, overexpression of PS2wt or PS2mut, but not PS1wt, inhibited general protein synthesis by 25–30% as determined by incorporation of [^{35}S]Met/Cys. A similar extent of inhibition was obtained in cultures transfected with PKR. Taken together, these results demonstrate that overexpression of PS2 inhibits overall protein synthesis in transfected cells.

Figures

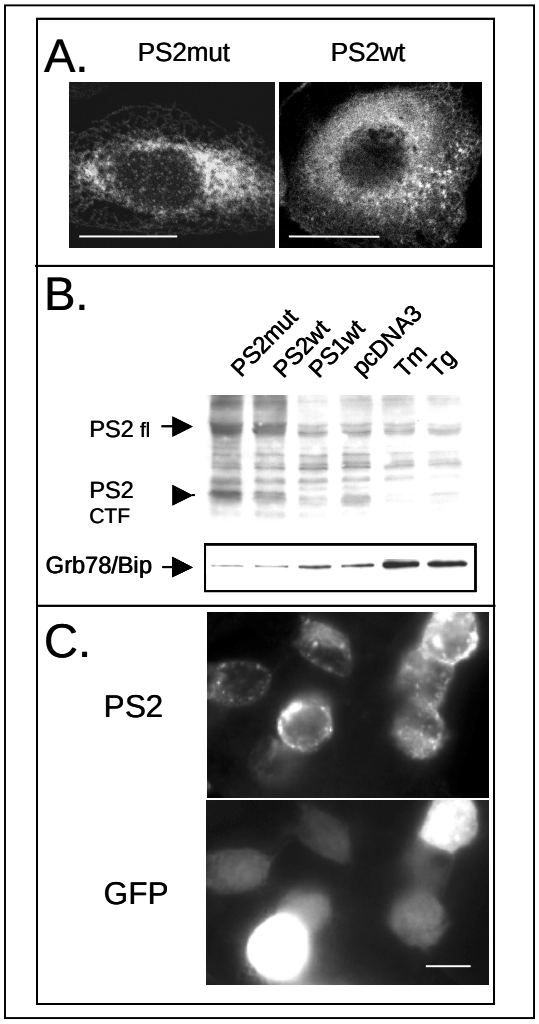

Figure 1. **Analysis of PS2 overexpression in transfected CHO and 293T cells**. (A), Subcellular localization of overexpressed PS2 proteins in CHO cells. CHO cells were transfected with PS2wt or PS2mut and stained after 24 h with anti-PS2 C-terminal specific monoclonal antibody (APS 26). Images were acquired on a laser scanning confocal microscope. Bar, 20 μm. (B), Immunoblot analysis of PS2 and Grb78/Bip expression. 293T cells were treated with tunicamycin (Tm) (10 μM) or thapsigargin (Tg) (2 μM) for 16 h, or co-transfected with GFP and PS2mut, PS2wt, PS1wt, or pcDNA3 expression vectors for 24 h. Cell lysates of these treatments (100 μg protein) were resolved by SDS–PAGE (12.5% polyacrylamide), and subjected to Western immunoblotting using anti-KDEL antibody or anti-PS2 loop (C-terminal) polyclonal antibody (28678), as described in Materials and Methods. Arrows indicate full-length PS2 (PS2 fl), C-terminal fragment PS2 (PS2 CTF), and Grb78/Bip. The figure shows the result of a representative experiment (one of 3 independent experiments). (C), Co-expression of PS2 and GFP in the same cell. CHO cells were co-transfected with PS2wt and GFP for 24 h. Cells overexpressing PS2 (PS2) were identified by immunofluorescent labeling using anti PS2 N-terminal rabbit polyclonal antibodies (44). GFP-positive cells (GFP) were identified using a fluorescein isothiocyanate filter set. Bar = 20 μm.

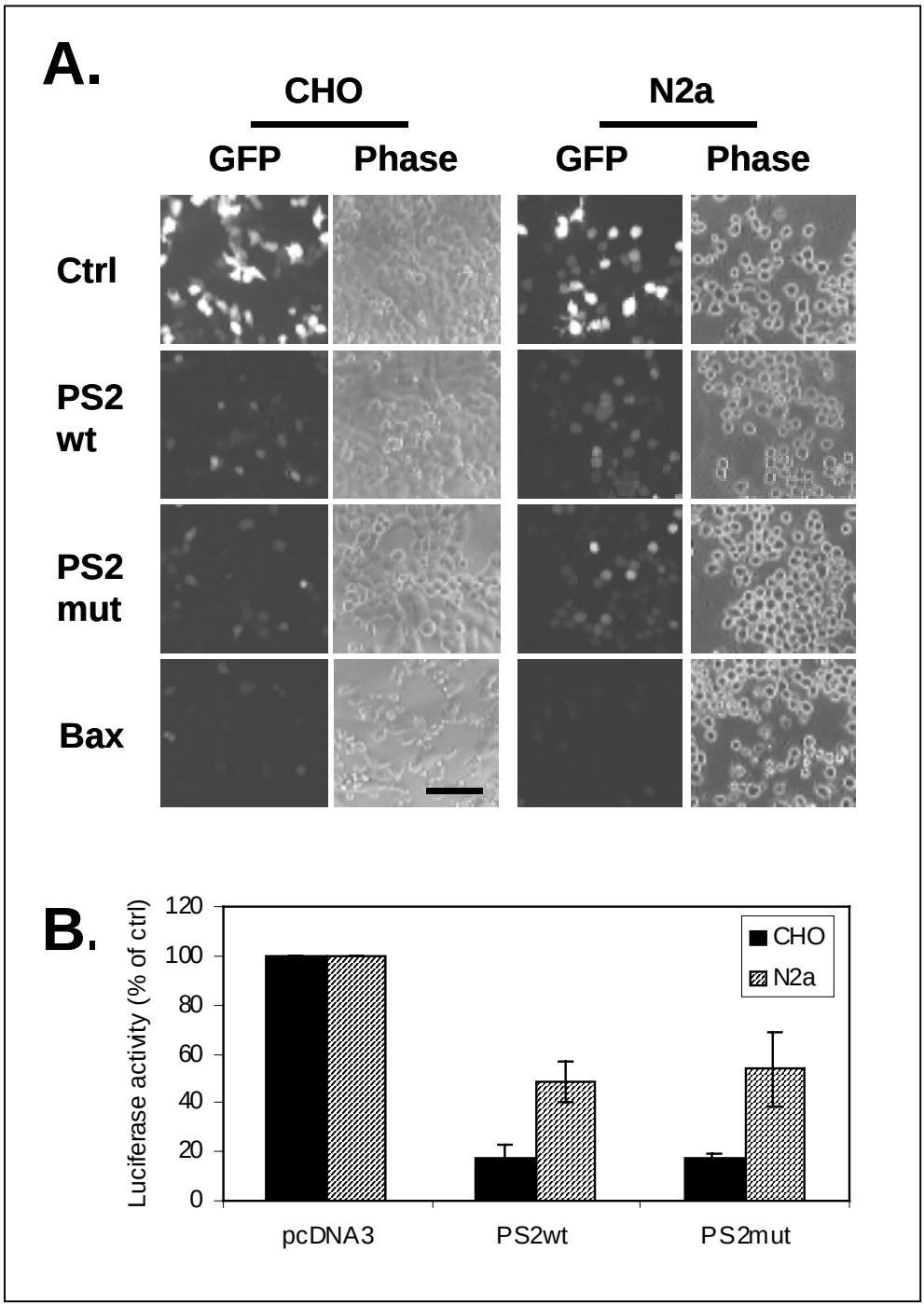

Figure 2. **PS2 overexpression diminishes the expression of co-expressed reporter genes.** (A) CHO and N2a cells were co-transfected with GFP and pcDNA3, PS2wt, PS2mut, or Bax expression vectors. After 24 h, the transfected cells were examined for GFP expression using fluorescein isothiocyanate and phase contrast filter sets. The results shown are of a representative experiment (one of 10 independent experiments). Bar = 100 μm. (B) CHO and N2a cells were co-transfected with luciferase and pcDNA3, PS2wt or PS2mut expression vectors. Luciferase activity was determined after 24 h as described in Materials and Methods. Results are expressed as the percentage of luciferase activity in PS2wt or PS2mut relative to the measured luciferase activity in cultures transfected with pcDNA3. Data shown are mean values ± SEM (bars)(n=4).

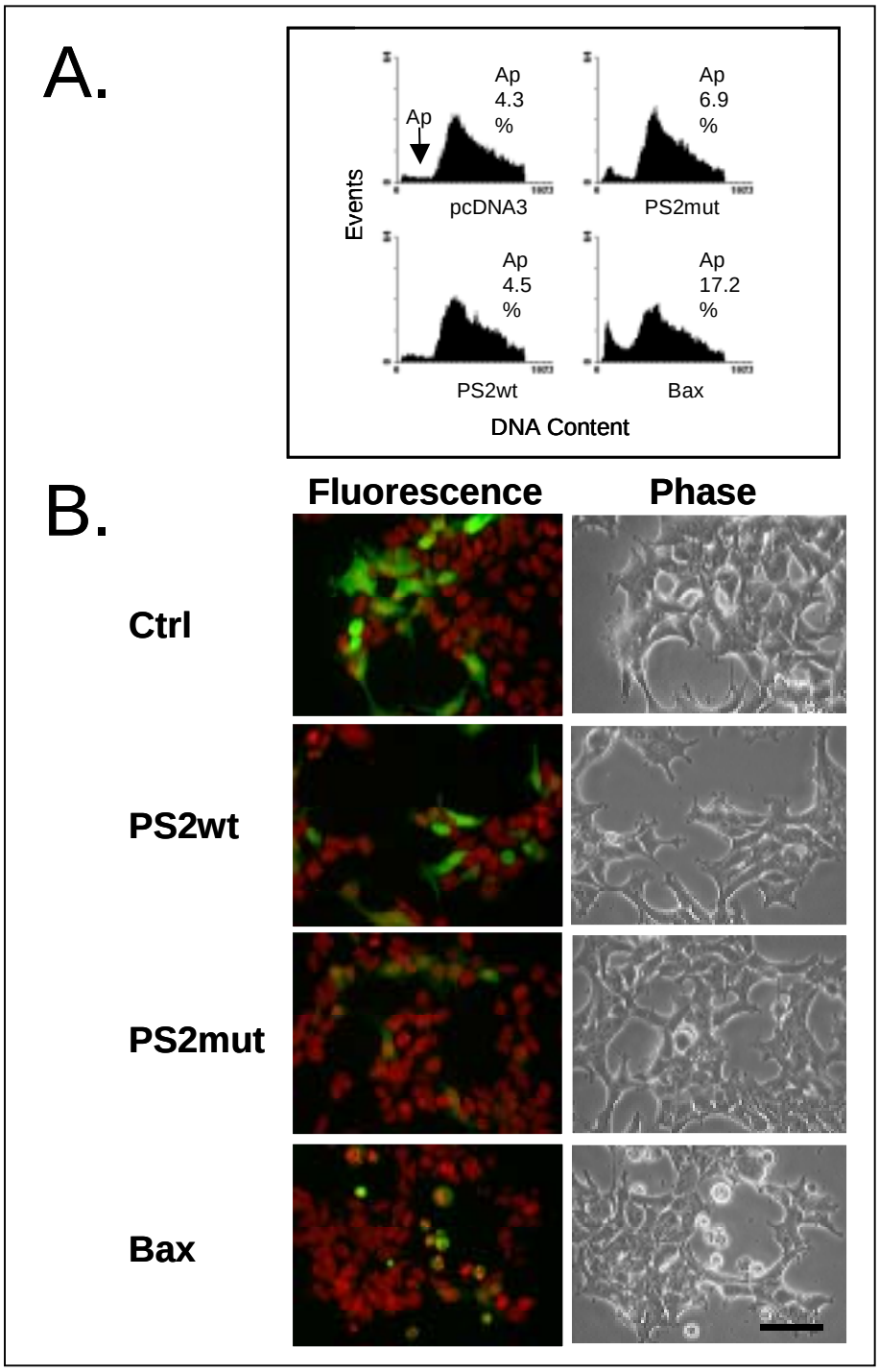

Figure 3. **Overexpression of PS2 does not induce apoptosis**. (A), DNA histograms of transfected CHO cells. CHO cells were co-transfected with GFP-F and PS2mut, PS2wt, Bax, or pcDNA3 expression vectors. After 24 h cells were harvested, stained with propidium iodide, and analyzed by flow cytometry. Data are presented as DNA frequency distribution histograms obtained from the GFP-positive cell population, as described in Materials and Methods. An arrow indicates the apoptotic cells (Ap). Data recorded in the figures show the percentages of apoptotic cell populations. (B), Hoechst 33342 staining of transfected 293T cells. 293T cells were co-transfected with GFP and PS2mut, PS2wt, Bax, or pcDNA3 (Ctrl) expression vectors. After 24 h the cells were stained with Hoechst 33342 (0.8 μg/ml) for 2 h to reveal the nuclei. GFP-positive cells and nuclear morphology were examined by fluorescence microscope with the appropriate filters. Data are shown as a phase-contrast image and as the merged image of the fluorescence staining in which the nuclei (Hoechst staining) appear red and the GFP appear green. Bar = 100 μm.

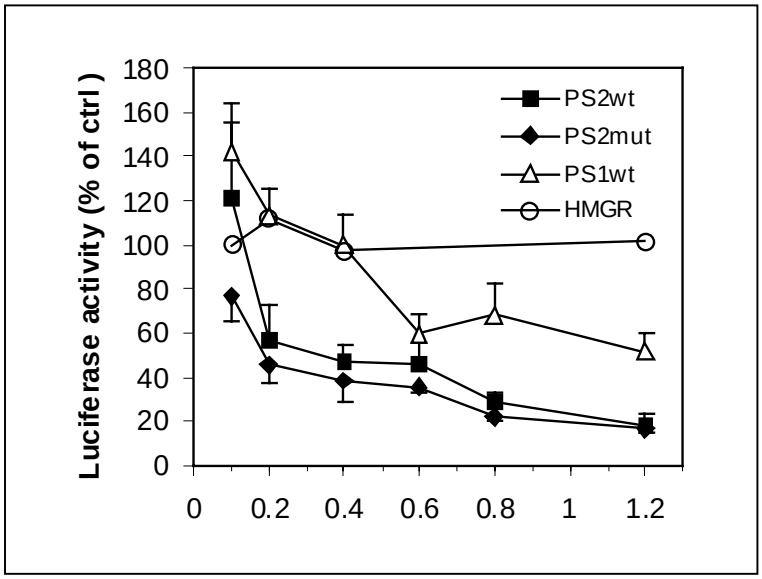

Figure 4. **Dose response of the effects of PS2wt, PS2mut, PS1wt, and HMGR on the co-expressed luciferase reporter gene**. CHO cells were co-transfected with luciferase (0.15 μg) and the indicated concentrations of pcDNA3 (Ctrl), PS2wt, PS2mut, PS1wt, or HMGR expression vectors. Luciferase activity was determined after 24 h as described in Materials and Methods. Results are expressed as percentage of luciferase activity in each PS2wt-, PS2mut-, PS1wt-, or HMGR-transfected culture relative to the measured luciferase activity in cultures transfected with pcDNA3. Data shown are mean values ± SEM (bars). The experiments (n =12, 8, 8, 4, 4, and 3 for 0.1, 0.2, 0.4, 0.8, 1, and 1.2 μg plasmids, respectively) were performed with different batches of plasmids.

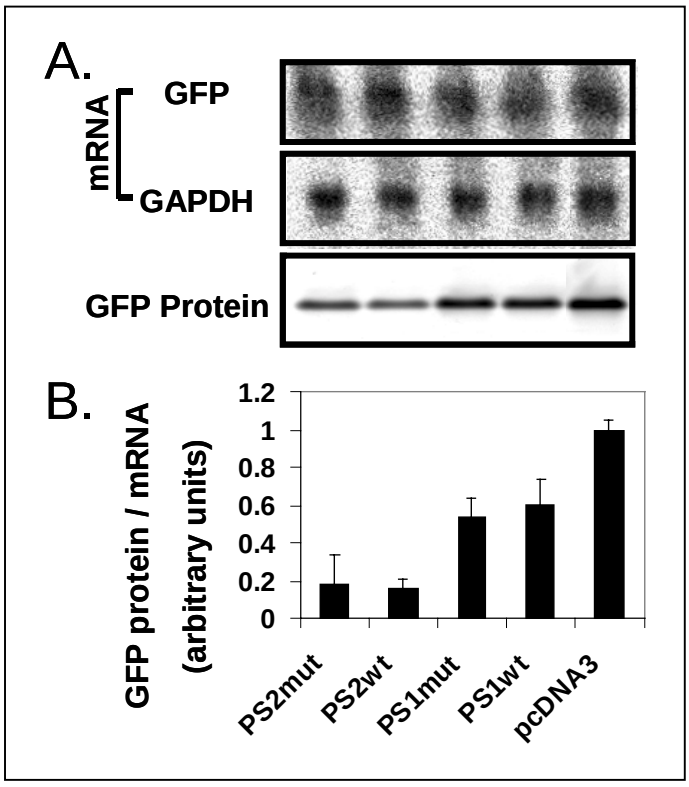

Figure 5. **PS2 overexpression reduces GFP protein but not GFP mRNA**. CHO cells were transfected with GFP and one of the indicated expression vectors. After 24 h, GFP mRNA and protein were determined (A). Northern blots (two upper panels) of total RNA extracted from transfected cells were probed with GFP or GAPDH DNA probes. GFP protein (third panel) was determined by measuring its fluorescence intensity directly from the gel (SDS–PAGE), using a FUJI FLA2000 fluorescence reader. Data shown are from a representative experiment (one of 7 independent experiments). (B), GFP mRNA and protein from 7 independent experiments, as described in A, were quantified. Data (mean values ± SD) are expressed as arbitrary units obtained from normalized amounts of GFP mRNA divided by the amounts of GFP protein.

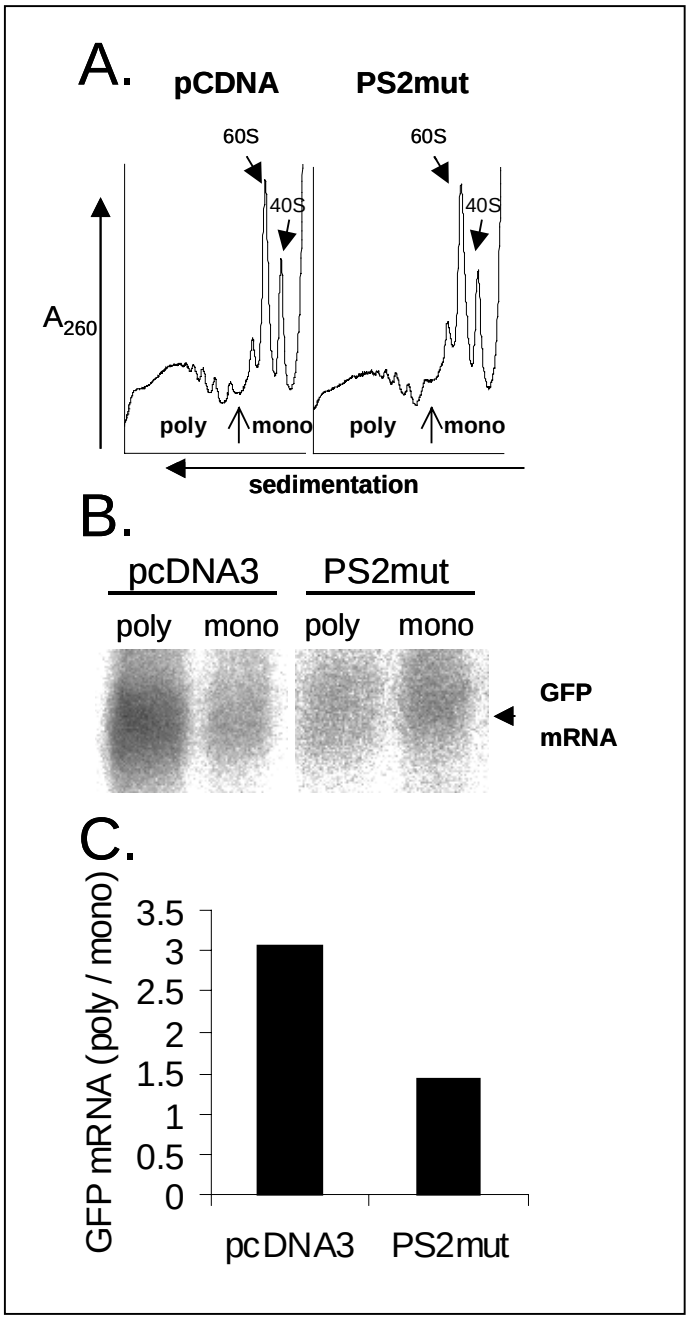

Figure 6. **PS2 overexpression reduces the amount of GFP mRNA associated with the polysomal fraction**. CHO cells were co-transfected with GFP and either PS2mut or pcDNA3 expression vectors. After 24 h, extracts were prepared and applied to 15–45% (wt/vol) linear sucrose gradients. The gradient was fractionated, and polysomal and monosomal fractions were detected by absorbence at OD_{260}. Typical profiles of such ribosomal separation is shown (A) for ribosomes obtained from pcDNA3 and PS2mut-transfected cells. The arrow indicates separation between the monosomal and the polysomal fractions. All polysomal fractions and all monosomal fractions were combined into two portions, the polysomal (poly) and the monosomal (mono) portions, respectively. Total RNA was prepared from these samples and GFP mRNA in each sample was determined by Northern blot analysis and hybridization with [^{32}P]GFP labeled probe (B). In addition, the filters were rehybridized with r-RNA probe to determine the amount of total RNA loaded in each sample (not shown). The intensities of the hybridization signals were measured by a FUJI FLA2000 Phosphor Imager. Quantitative analysis of these hybridization signals is shown in C. GFP mRNA in the monosomal and polysomal samples were normalized to the amounts of ribosomal RNA in each sample and to the amount of RNA in each sample expressed as a percentage of the total RNA. Results are expressed as the ratio of normalized GFP mRNA in polysomes to the normalized GFP mRNA in monosomes. Data shown are from a representative experiment (one of 2 independent experiments).

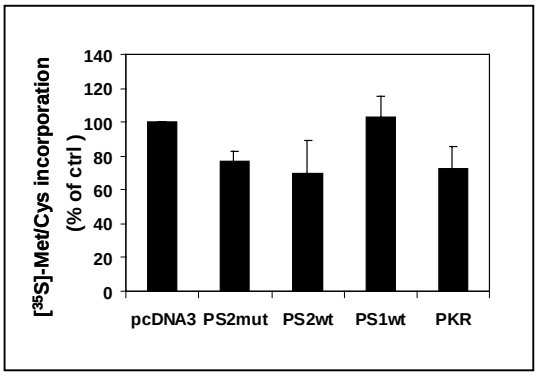

Figure 7. **PS2 overexpression reduces endogenous protein synthesis**. CHO cells were transfected with the indicated expression vectors. After 24 h, the cells were labeled with [^{35}S]Met/Cys for 3 h. Incorporation of radioactivity into a trichloroacetic acid (10%)-insoluble fraction of the cells was measured. Results are expressed as the percentage of [^{35}S]Met/Cys incorporated into pcDNA3-transfected cells (Ctrl). Data are mean values ± SEM (bars) (n = 4).

B5. The effects of cholesterol on the metabolism of the amyloid precursor protein and on amyloids genesis (Heidelberg)

Though the primary function of the amyloid precursor (APP) *in vivo* remains unclear, it is generally accepted that APP is sequentially processed by several proteolytic events. Cleavage of the full-length precursor by α-secretase creates APPαsec, which is released into the medium, leaving behind a short membrane-bound carboxy-terminal fragment (αCTF). Less frequently, the holoprotein may be cleaved at a slightly more N-terminal site, generating βCTF and APPβsec. APP-CTFs can be further processed by γ-secretase. This second cleavage event occurs within the membrane region of the carboxy-terminal stumps and requires a complex containing the multi-transmembrane spanning proteins PS1 or 2 and nicastrin. Cleavage at the γ-site of βCTF generates the 4 kDa-fragment Aβ, which represents a major component of amyloid plaques in Alzheimer´s disease (AD). Further cleavage of αCTF yields the non-amyloidogenic peptide p3.

Increasing evidence suggests a role for cholesterol in the metabolism of APP. Carriers of the apoE4-allele of the apolipoprotein E are predisposed to an earlier onset for developing sporadic AD (4) and high cholesterol diet accelerated Ab-deposition in transgenic mice(6). The importance of the low-density lipoprotein (LDL) receptor-family in mediating cellular ApoE uptake as well as a role for LRP in increasing Aβ-production by enhancing the endocytosis of APP suggest an involvement of cholesterol internalization processes in APP-metabolism. Moreover, suppression of cellular cholesterol neosynthesis by inhibiting HMG-CoA-reductase strongly reduces the formation of Aβ-species *in vivo* and *in vitro* (5,7,8).

B5.1 Cholesterol dependent parallel but independent inhibition of ß and γ-secretase
(Bergmann et al. ms in preparation)

The simultaneous inhibition of β-and γ-secretase activity may be due to the same, or the result of two independent mechanisms. The difference between the strong reduction in Aβ generation from APP695 and the weaker inhibition of Aβ generation from C99 indicates the presence of two additive mechanisms. To further address this question we used another SFV-construct termed SP-C111 (9). Unlike full length APP, this N-terminally truncated construct does not require previous secretase cleavage in order to allow γ-secretase cleavage to occur, giving raise to a 5,5 kDa fragment. However, in this

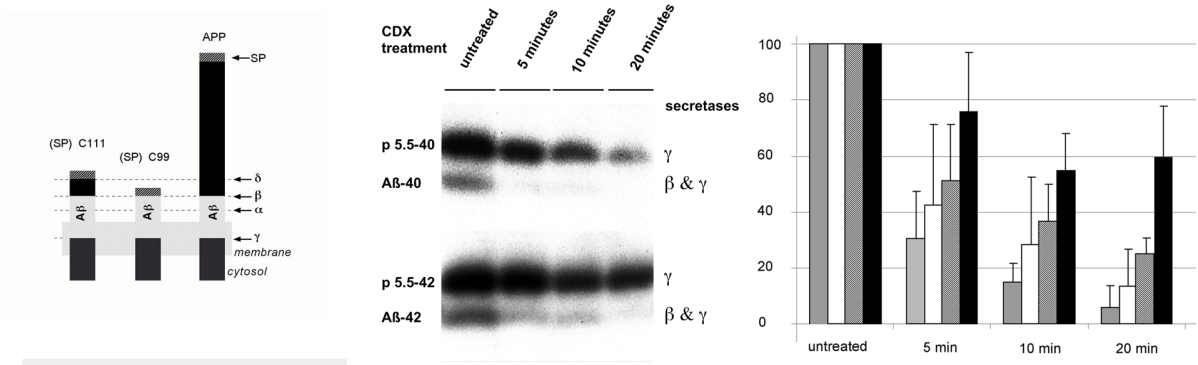

Figure 8. Independence of β-and γ-secretase cleavage inhibition by reduced cholesterol levels
Cell lysates from mixed cortical neurons were immunoprecipitated with antibodies G2-10 and G2-11 and detected with antibody W0-2. In order to simultaneously assess β- and γ-cleavage independently of one another and in their sequential order, construct C111 was analyzed. The upper band of an apparent molecular weight of 5,5 kDa termed p5,5 represents γ-cleavage activity only, whereas the lower band represents Aβ generated by β-and γ-secretase activity as indicated. The β-and γ-secretase products, Aβ40 and Aβ42, are both very sensitive towards peripheral cholesterol depletion by methyl-β-cyclodextrin. The same holds true for the γ-secretase only product, p5,5-40, whereas p5,5-42 is much less affected by

construct β-secretase cleavage may take place normally yielding a 4 kDa fragment which is identical to Aβ, when followed by γ-secretase cleavage (9). Thus with this construct it is possible to analyze β- and γ-secretase activity in parallel, independent of each other or in their sequential order. The γ-secretase 40 activity giving raise to p5,5 is strongly affected by peripheral cholesterol depletion. The same holds true for the „β-secretase 40"-γ-secretase 40 product p4 which is identical to Aβ40 and which is strongly decreased. However, γ-secretase 42 activity is less influenced by peripheral cholesterol depletion as shown by relatively high levels of its product p5.5. Interestingly, the „β-secretase 42"-γ-secretase 42 product p4 which is identical to Aβ42 is very sensitive to cholesterol depletion throughout increasing extraction times in all cases as compared to untreated cells). We conclude from this that β-secretase activity resulting in Aβ42 or Aβ40 products is very sensitive to and γ-secretase 42 activity is largely resistant towards reduced peripheral cholesterol levels. Thus, it is highly likely that the mechanism for γ-secretase 42 inhibition is different from the mechanism for β-secretase 42 inhibition.

B5.2 Inverse effects of cholesterol treatment on APP-secretases

(Runz et al. 2002)

In the previous work we were able to show independent but parallel inhibition of APP secretases. We were now interested to extend this finding further to see whether it is possible to target secretases specifically.

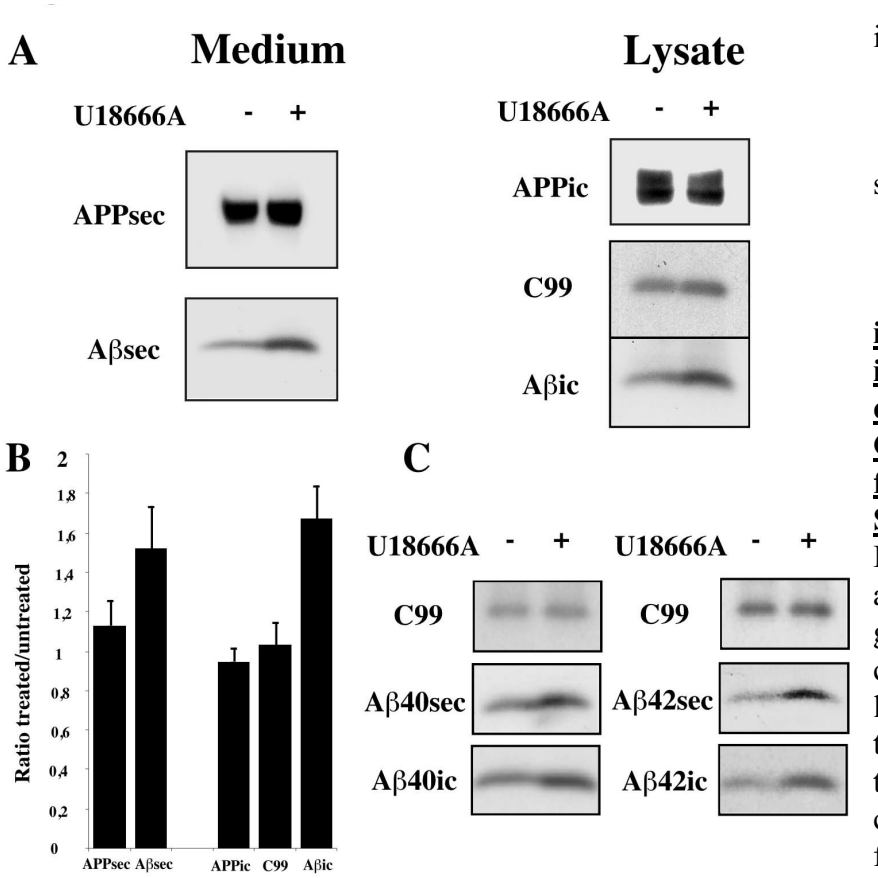

Figure 9. U18666A increases intracellular and secretory Aß-levels in SP-C99-transfected SH-SY5Y cells Human SH-SY5Y-neuroblastoma cells stably transfected with APP-C-terminal fragment SP-C99 were incubated for 24 hours with 50 mg/ml LDL in the presence (+) or absence (-) of 3 mg/ml U18666A. (a) Conditioned medium and cell-lysates were immuno-precipitated with antibody W02 followed by Western Blot detection with W02. (b) Quantification of intracellular (ic) and secreted (sec) endogenous APP, C99 and overall Aβ-levels (n = 5 experiments). Depicted are ratios of signal-intensities from U18666A-treated versus untreated cells. (c) Medium and lysates of SH-SY5Y cells were immunoprecipitated with antibodies G2-10 and G2-11 specific for Ab40 and Ab42 respectively and detected with W02. Western Blots with W02 show effects of U18666A-treatment on secretory and

U18666A increases Aβ-levels in SH-SY5Y cells expressing APP-Carboxy- terminal fragment fragment SP-C99.

In view of the association of Aβ-generation with cellular cholesterol-levels we speculated that cholesterol-trafficking or cholesterol uptake from extracellular

sources may affect γ-cleavage of APP. Generation of Aβ from full-length APP requires the sequential cleavage by two proteolytic activities. Cleavage by γ-secretase depends on the prior production of APP-βCTF, which is generated by β-secretase. Using a truncated form of APP, SP-C99, instead of the full-length molecule, which acts as an immediate precursor for Aβ and as a direct substrate for γ-secretase allows an isolated assessment of γ-secretase-activity and obviates β-secretase cleavage for Aβ-generation(10). β-CTF-like constructs have previously been shown as suitable models for studying γ-cleavage in the absence of β-cleavage(11).

With the aim to determine the effects of U18666A-mediated disruption of cellular cholesterol-transport on γ-secretase cleavage, we stably transfected SH-SY5Y cells with SP-C99 and exposed these cells to LDL-enriched culture medium in the presence or absence of 3 μg/ml U18666A. Notably, ApoE protein is an important constituent of cholesterol containing LDL. Western blot detection showed that levels of endogenously synthesized secretory human APP (APPsec) in conditioned medium from U18666A-treated cells were largely unaffected compared to controls, while secretory Aβ-levels (Aβsec) were markedly elevated. Similarly, while there was no major difference in C99-levels, the substrate for γ-secretase upon co-translational cleavage of the signal peptide from SP-C99, as well as in the levels of endogenously synthesized APP (APPic) in cell lysates, a strong increase in overall intracellular Aβ

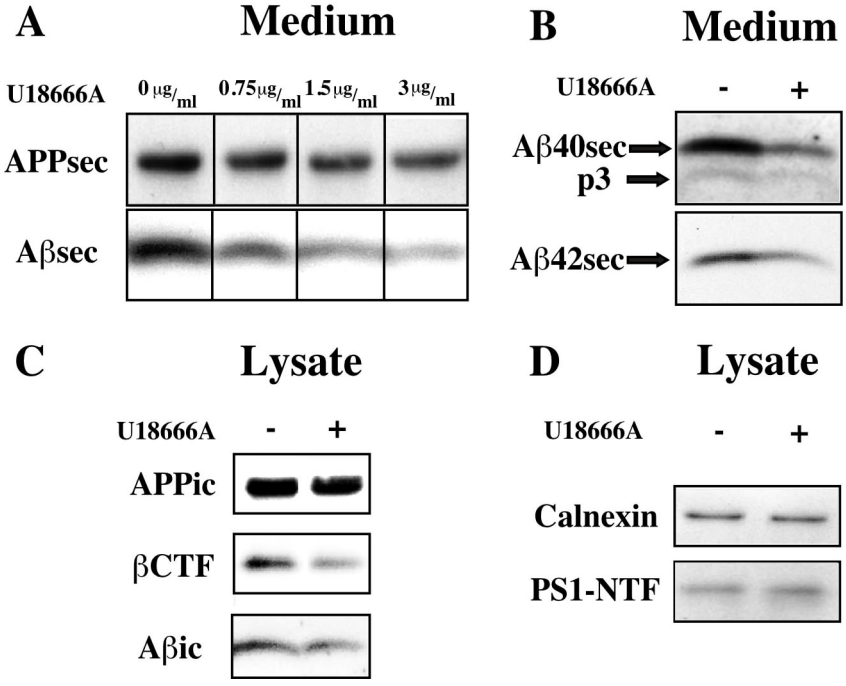

Figure 10. U18666A decreases β-secretase activity in cortical neurons expressing APP695 (a) SFV-infected mature rat cortical neurons were incubated for 8 hours with LDL at different concentrations of U18666A. Conditioned medium was immunoprecipitated with W02 followed by Western Blot detection with W02. (b) Immunoprecipitations of conditioned media from neurons exposed to LDL and either 0.75 μg/ml U18666A (+) or not (-) with antibodies G2-10 or G2-11 were detected with G2-10 to visualize secretory Aβ40 and p3, or W02 for the detection of secretory Aβ42 respectively. (c) W02-immuno-precipitation of respective neuronal lysates detected with W02. (d) Western Blot of neuronal lysates from U18666A-treated (+) and untreated (-) neurons with anti-calnexin antibody and antibody 95.23 against PS1-NTF.

(Aβic) was observed. Quantification revealed a significant increase in secretory Aß-species compared to controls whereas no major changes were found for secretory APP (1.56±0.221, n=5 for Ab, $p<0.01$ compared to 1.155±0.134, n=5 for APP). While intracellular APP (from endogenous APP) and C99-levels (from transfected SP-C99) were largely unaffected (0.969±0.074, n=5 for APP and 1.059±0.118, n=5 for C99 respectively), neuroblastoma cells exposed to U18666A showed a highly significant

increase in intracellular Ab-levels. Compared to untreated cells, total intracellular Ab-levels showed a 1.7 fold increase (1.715±0.172, n=5, $p<0.0005$) reflecting a strong upregulation of γ-secretase activity in response to an altered subcellular cholesterol-distribution. Because of this strong enlargement of overall intracellular and secreted Aβ-pools, we were interested, which of the major Aβ-species might contribute to this effect. At equal expression levels of C99, we found a remarkable increase in both Aβ40 and Aβ42 in cells exposed to U18666A compared to controls. This increase was prominent for secretory as well as for intracellular forms of both Aβ-species and appeared to be more pronounced for Aβ42 than for Aβ40.

These results demonstrate an effect of impaired cholesterol-trafficking on γ- secretase-activity resulting in an increased formation of Aβ-species.

Inhibition of cholesterol- trafficking in neurons expressing full-length APP affects proteolytic processing by β-secretase

Unlike SP-C99, full-length APP requires the preceding cleavage by β-secretase to act as a substrate for γ-secretase. To analyze Aβ-generation in cells expressing full-length APP, primary cultures of mixed cortical neurons were infected with recombinant Semliki-Forest Virus (SFV) encoding for human APP695. This expression system has widely been used to study sorting and processing of APP in neuronal cells and did not affect neuronal viability within the duration of our experiments. Infected neurons were exposed for 8 hours to LDL in the presence or absence of U18666A. Application of U18666A to cortical neurons in culture resulted in a dose-dependent reduction in Aβ-secretion. In contrast, secretion of APP decreased notably less than secretion of Aβ, arguing that diminished Aβ-levels in the medium did not result from a general disruption of protein secretion at higher inhibitor concentrations. At concentrations of 0.75 μg U18666A/ml culture medium, levels of secretory Aβ decreased by about 50% while APP-levels remained essentially unaffected (0.491±0.094, n=4, $p<0.01$ for Aβsec; 0.958±0.08, n=4 for APPsec). These observations were independent from the expression system, as very similar effects could be obtained for SH-SY5Y cells stably expressing APP695 (data not shown). A diminished secretion was prominent for both, Aβ40 and Aβ42, indicating that none of the major γ-secretase activities was perturbed in favor to the other. Reduced secretion of Aβ could not be explained by an increase in the α-secretory cleavage pathway of APP(12), as we did not observe a compensatory upregulation of p3-levels. Therefore, we determined the levels of APP-proteolytic products and related proteins in lysates of U18666A-treated and untreated neurons. While intracellular APP-expression as well as expression levels of PS1 and calnexin were unperturbed, we found remarkably less βCTF upon exposure to U18666A compared to controls. Quantification revealed a decrease in βCTF-levels to an almost similar extent as for secretory Aβ-levels (0.524±0.203, n=4, $p< 0.05$ for βCTF; 0.96±0.244, n=4 for APPic). We conclude, that a reduced β- rather than γ-cleavage is responsible for the reduction in Aβ-secretion in APP-expressing neurons exposed to U18666A.

Relevance of cholesterol trafficking pathways to presenilin subcellular localization.

U1866A treatment blocks cholesterol trafficking at the level of the rab7/NPC1 compartment which is often reffered to as the “cholesterol sorting compartment”.

Presenilin is in its vast majority targeted to the ER and to a minor extend to the early Golgi apparatus. Several reports showed evidence that minor amounts of presenilin may be present at other cellular compartments as well but remained a matter of discussion. Since presenilines are absolutely essential for g-secretase activity it is very difficult to understand how g-secretase activity can be observed in other compartments than the early secretory pathway. However, this is clearly the case. Since we observed increased g-secretase activity upon U18666A treatment, we investigated the effect on presenilin processing and localization. We did not observe any obvious changes in presenilin processing but we did observe a drastic alteration in the subcellular localization. Upon treatment with U18666A presenilin 1 and presenilin 2 localized to small vesicular structures positive for rab7, but negative for markers of late endosomal compartments. However, these presenilin rich vesicles were directly surrounded by large amounts of vesicular structures positive for late endosomal markers and likely due to the U18666A treatment, also rich in cholesterol. Since we had observed increased Aß42 production from C99 in treated cells we analyzed for possible g-secretase activity in the presenilin rich compartments. Indeed strongly accumulated Aß42 was found to colocalize to the rab7 marked presenilin rich vesicles.

These data indicate that, at least partially, no spatial paradox exists, but rather that presenilin and C99 transiently engage, resulting in g-secretase cleavage. U18666A treatment traps both proteins during trafficking and enriches them into a compartment otherwise of low presenilin content. However, such a brief interaction during trafficking, would be sufficient for g-secretase activity.

B5.3 APP dimerization as factor in Aß generation

Oligomeric states of APP695-K624C mutant APP and Aß production thereof. Dimerization of APP695-K624C mutant APP is mediated by the presence of the disulfide bond in the juxta-membrane domain of APP. Western blotting with monoclonal antibody 22C11 of the immuno-precipitated Cys-mutant APP (APP695-K624C) but not the wild-type APP from lysates of stably transfected SY5Y cells reveals dimers (~220kDa; myc-/myc-APP, open arrow) under non-reducing conditions (-DTT), separated on 7-10% acrylamide gradient gels. In the presence of DTT, APP dimers are converted to monomers (lane APP695-K624C, +DTT; myc-APP,

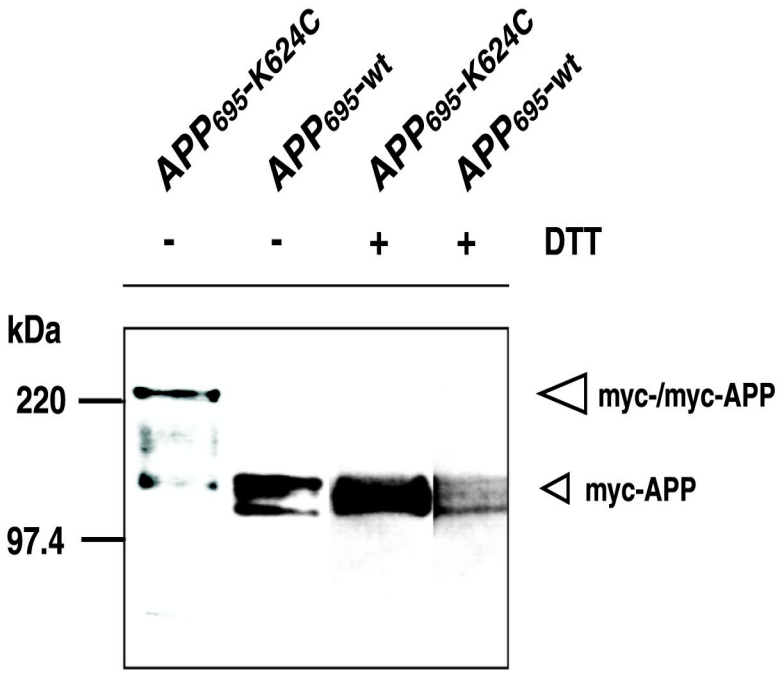

Figure 11. Dimerization of APP

open arrow head) migrating at ~110kDa and co-migrating with endogenous forms of APP from SY5Y cells. Amyloid Aß was immunoprecipitated with monoclonal antibody W0-2 from the medium of SY5Y cells transfected as described, separated on NuPAGE-gels under non-reducing (lanes –DTT/APP695-K624C, -DTT/APP695-wt) or reducing conditions (+DTT/APP695-K624C, +DTT/APP695-wt) and analyzed by Western blotting with the same antibody W0-2 after cutting the filter. Under non-reducing conditions (-DTT), Aß dimers (~8.5kDa) can be precipitated from cell culture supernatant of transfected APP695-K624C SY5Y cells. In the presence of DTT, Aß dimers are converted to monomers (lane APP695-K624C, +DTT) migrating at ~4.5kDa. Quantification of Aß production was based on the average of three replicates. Note the faint bands of Aß derived from endogenously expressed APP.

Oligomerization of N-terminally extended APP forms was assessed in lysates from transiently transfected COS-7 cells after immunoprecipitation with polyclonal anti-APP18-350 (40090) and Western blotting with 22C11 under non-reducing conditions. From top to bottom, the positions of myc-K624C/GFP-K624C APP695 heterodimers from doubly transfected cells (closed arrow),

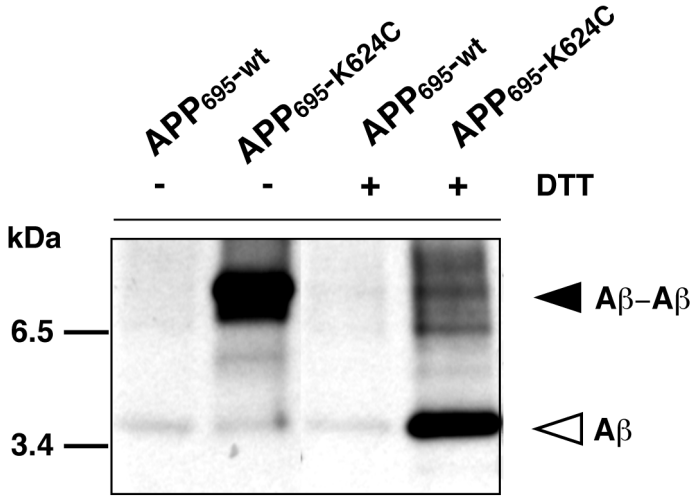

Figure 12. APP dimerization and Aβ

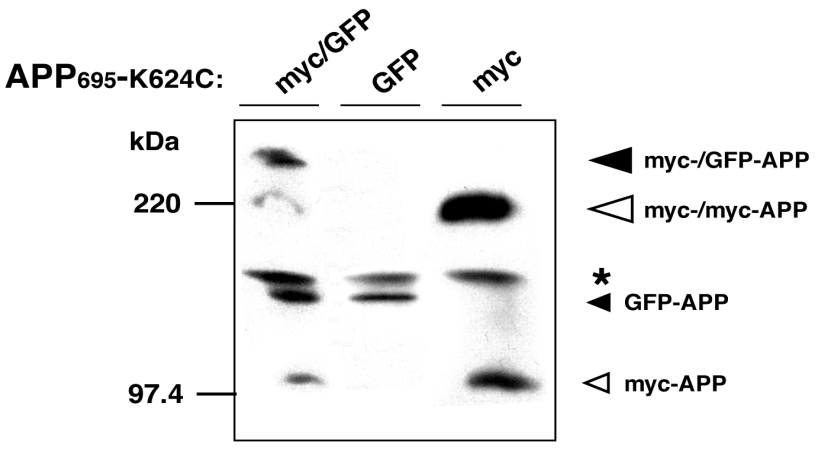

Figure 13. Oligomerization of N-terminally extended forms of APP

myc-K624C APP695 homodimers (open arrow) in myc-K624C APP695 homodimers myc-K624C/GFP-K624C doubly and myc-K624C transfected cells, endogenous KPI forms of APP from COS-7 cells (star) in all lines, monomeric GFP-K624C (closed arrow head) in myc-K624C/GFP-K624C and GFP-K624C transfected cells and monomeric myc-K624C (open arrow head) in myc-K624C/GFP-K624C and myc-

K624C transfected cells are shown. Note that homodimers of GFP-K624C were not detected.

Conclusions:
Taken together our data clearly show a triangular connection between APP, PS and ApoE with the unexpected molecule cholesterol as their center part. All of those proteins have important and additional functions beyond their cholesterol interactions, however, in the case of the pathological events during the development of Alzheimer's disease it appears that cholesterol is able to build a detrimental link between these proteins resulting in increased Aß42 production. Cholesterol drastically alters function, activity or respectively protein stability. It is fascinating to see how a slight change in the delicate balance of these molecules can result in an enhanced response in Aß production several steps along this cascade later. E.g. differences in ApoE regulated cholesterol uptake (function) results in increased presenilin dependent g-secretase activity (activity), which in turn results in increased degradation of APP (protein stability) and thus in increased Aß42 production. Depending on the very nature of this change the net result can be easily manipulated in both directions – either increased Aß42 - or alternatively, decreased Aß42 production. The former helping us to understand a little bit better what makes the difference between disease and health, the other to develop new aproaches towards treatment and prevention of disease.

B6. References

1. Kang, J., Lemaire, H. G., Unterbeck, A., Salbaum, J. M., Masters, C. L., Grzeschik, K. H., Multhaup, G., Beyreuther, K., and Muller Hill, B. The precursor of Alzheimer's disease amyloid A4 protein resembles a cell-surface receptor. *Nature* **325,** (6106)**,** 733-6 (1987)

2. Selkoe, D. J., Yamazaki, T., Citron, M., Podlisny, M. B., Koo, E. H., Teplow, D. B., and Haass, C. The role of APP processing and trafficking pathways in the formation of amyloid beta-protein. *Ann N Y Acad Sci* **777,** 57-64 (1996)

3. Masters, C. L., Simms, G., Weinman, N. A., Multhaup, G., McDonald, B. L., and Beyreuther, K. Amyloid plaque core protein in Alzheimer disease and Down syndrome. *Proc Natl Acad Sci U S A* **82,** (12)**,** 4245-9 (1985)

4. Corder, E. H., Saunders, A. M., Strittmatter, W. J., Schmechel, D. E., Gaskell, P. C., Small, G. W., Roses, A. D., Haines, J. L., and Pericak-Vance, M. A. Gene dose of apolipoprotein E type 4 allele and the risk of Alzheimer's disease in late onset families. *Science* **261,** 921-923 (1993)

5. Fassbender, F., Simons, M., Bergmann, C., Stroick, M., Lütjohann, D., Keller, P., Runz, H., Kühl, S., Bertsch, T., von Bergmann, K., Hennerici, M., Beyreuther, K., and Hartmann, T. Simvastatin strongly reduces Alzheimer's disease Ab42 and Ab40 levels in vitro and in vivo. *Proc Natl Acad Sci U S A* **98,** (10)**,** 5856-61 (2001)

6. Refolo, L. M., Pappolla, M. A., Malester, B., LaFrancois, J., Bryant-Thomas, T., Wang, R., Tint, G. S., Sambamurti, K., and Duff, K. Hypercholesterolemia accelerates the Alzheimer's amyloid pathology in a transgenic mouse model. *Neurobiol Dis* **7,** (4)**,** 321-31. (2000)

7. Simons, M., Keller, P., De Strooper, B., Beyreuther, K., Dotti, C. G., and Simons, K. Cholesterol depletion inhibits the generation of beta-amyloid in hippocampal neurons. *Proc Natl Acad Sci USA* **95,** 6460-6464 (1998)

8. Frears, E. R., Stephens, D. J., Walters, C. E., Davies, H., and Austen, B. M. The role of cholesterol in the biosynthesis of beta-amyloid. *Neuroreport* **10,** (8)**,** 1699-705 (1999)

9. Tienari, P. J., De Strooper, B., Ikonen, E., Simons, M., Weidemann, A., Czech, C., Hartmann, T., Ida, N., Multhaup, G., Masters, C. L., Van Leuven, F., Beyreuther, K., and Dotti, C. G. The beta-amyloid domain is essential for axonal sorting of amyloid precursor protein. *Embo J* **15,** (19)**,** 5218-29 (1996)

10. Dyrks, T., Dyrks, E., Monning, U., Urmoneit, B., Turner, J., and Beyreuther, K. Generation of beta A4 from the amyloid protein precursor and fragments thereof. *FEBS Lett* **335,** (1)**,** 89-93. (1993)

11. Lichtenthaler, S. F., Wang, R., Grimm, H., Uljon, S. N., Masters, C. L., and Beyreuther, K. Mechanism of the cleavage specificity of Alzheimer's disease gamma- secretase identified by phenylalanine-scanning mutagenesis of the transmembrane domain of the amyloid precursor protein. *Proc Natl Acad Sci U S A* **96,** (6)**,** 3053-3058 (1999)

12. Kojro, E., Gimpl, G., Lammich, S., März, W., Fahrenholz, F. Low cholesterol stimulates the nonamyloidogenic pathway by its effect on the alpha-secretase ADAM 10. *Proc Natl Acad Sci USA* **98,** (10)**,** 5815-5820 (2001)

Own publications from this work:

Runz H, Rietdorf J, Tomic I, de Bernard M, Beyreuther K, Pepperkok R, and Hartmann T. Inhibition of intracellular cholesterol transport alters presenilin localization and amyloid precursor protein processing in neuronal cells. *J Neurosci.* 2002 Mar 1;22(5):1679-89.

Fassbender, F., Simons, M., Bergmann, C., Stroick, M., Lütjohann, D., Keller, P., Runz, H., Kühl, S., Bertsch, T., von Bergmann, K., Hennerici, M., Beyreuther, K., and Hartmann, T. Simvastatin strongly reduces Alzheimer’s disease Ab42 and Ab40 levels in vitro and in vivo. *Proc Natl Acad Sci U S A* **98,** (10)**,** 5856-61 (2001)

Scheuermann S, Hambsch B, Hesse L, Stumm J, Schmidt C, Beher D, Bayer TA, Beyreuther K, Multhaup G. Homodimerization of amyloid precursor protein and its implication in the amyloidogenic pathway of Alzheimer's disease. *J Biol Chem.* 2001 Sep 7;276(36):33923-9.